



HHS Public Access

Author manuscript

Clin Biomech (Bristol, Avon). Author manuscript; available in PMC 2016 August 01.

Published in final edited form as:

Clin Biomech (Bristol, Avon). 2015 August ; 30(7): 748–754. doi:10.1016/j.clinbiomech.2015.04.010.

An Approach for Determining Quantitative Measures for Bone Volume and Bone Mass in the Pediatric Spina Bifida Population

Rachel E. Horenstein, M.S.¹, Sandra J. Shefelbine, Ph.D.², Nicole M. Mueske, M.S.³, Carissa L. Fisher, B.S.³, and Tishya A.L. Wren, Ph.D.^{1,3}

¹Department of Biomedical Engineering, University of Southern California, Los Angeles CA, United States

²Department of Mechanical and Industrial Engineering, Northeastern University, Boston MA, United States

³Children's Orthopaedic Center, Children's Hospital Los Angeles, Los Angeles CA, United States

Abstract

Background—The pediatric spina bifida population suffers from decreased mobility and recurrent fractures. This study aimed to develop a method for quantifying bone mass along the entire tibia in youth with spina bifida. This will provide information about all potential sites of bone deficiencies.

Methods—Computed tomography images of the tibia for 257 children ($n=80$ ambulatory spina bifida, $n=10$ non-ambulatory spina bifida, $n=167$ typically developing) were analyzed. Bone area was calculated at regular intervals along the entire tibia length and then weighted by calibrated pixel intensity for density weighted bone area. Integrals of density weighted bone area were used to quantify bone mass in the proximal and distal epiphyses and diaphysis. Group differences were evaluated using analysis of variance.

Findings—Non-ambulatory children suffer from decreased bone mass in the diaphysis and proximal and distal epiphyses compared to ambulatory and control children ($P < 0.001$). Ambulatory children with spina bifida showed statistically insignificant differences in bone mass in comparison to typically developing children at these sites ($P > 0.5$).

Interpretation—This method provides insight into tibial bone mass distribution in the pediatric spina bifida population by incorporating information along the whole length of the bone, thereby providing more information than dual-energy x-ray absorptiometry and peripheral quantitative computed tomography. This method can be applied to any population to assess bone mass distribution across the length of any long bone.

Corresponding Author Contact: Rachel Horenstein, Northeastern University, 360 Huntington Avenue, Egan 260, Boston, MA 02115, 617-373-3850, horenstein.r@husky.neu.edu.

Publisher's Disclaimer: This is a PDF file of an unedited manuscript that has been accepted for publication. As a service to our customers we are providing this early version of the manuscript. The manuscript will undergo copyediting, typesetting, and review of the resulting proof before it is published in its final citable form. Please note that during the production process errors may be discovered which could affect the content, and all legal disclaimers that apply to the journal pertain.

Keywords

spina bifida; myelomeningocele; bone density; bone mass; image analysis

1. Introduction

Spina bifida is a birth defect that results from incomplete closure of the spinal column during fetal development. Children with spina bifida suffer from decreased mobility secondary to weakness or paralysis of lower extremity muscles, leading to atypical loading of the legs. As a result, reduced bone mineral density (BMD) is among the more common complications in children with spina bifida [1]. Reduced bone density may cause recurrent fractures of the lower extremities that are more numerous and frequent than those in typically developing children [1]. Children with spina bifida often undergo repeated surgeries and immobilizations, which in turn decrease bone density and increase fracture risk [2–3]. It has been reported that children with higher lesion levels and lower ambulatory ability have a higher risk of fractures than more functional children with spina bifida [3]. The high risk of fracture in children with spina bifida appears to be due to decreased muscle activity in their paralyzed lower extremities and the resulting insufficient axial loading of these limbs [4]. The distal tibia and femur are the most common fracture sites in children with spina bifida, with fractures in the proximal tibia and femur occurring less commonly [4].

To date, there are no commonly used analytic methods for providing information about distribution of bone mass across the entire length of a long bone. Current techniques for measuring BMD rely most commonly on dual-energy x-ray absorptiometry (DXA) and, to a lesser extent, peripheral quantitative computed tomography (pQCT). DXA provides a projected areal measure of BMD and therefore cannot provide a complete adjustment for bone size [5]. This limitation has consequences for comparing BMD across individuals of different physical sizes [6–8], including children with spina bifida who typically have short stature in comparison to typically developing peers [9]. This short stature may result in a biased DXA result since lower BMDs are anticipated in shorter individuals due to their inherently smaller bones [10]. A further limitation of DXA is that it cannot differentiate between cortical and trabecular bone [6]. As an alternative to DXA, pQCT can provide three-dimensional information, but it can only be used to image distal sites due to the small size of the gantry, which cannot accommodate larger, more proximal sites. In addition, the use of pQCT is limited because the field of view of current pQCT systems cannot accommodate the entire length of a long bone and therefore cannot provide a means to measure the whole bone for deficiencies in the pediatric population, including children with spina bifida. Furthermore, current standards for analyzing acquired BMD datasets do not necessarily include analysis of BMD information across the entire length of a bone, which may lead to incomplete results and conclusions.

The purpose of this study was to assess bone mass and bone area (BA) along the entire length of the tibia in children with spina bifida. The ability to examine an entire long bone is advantageous because it provides information about all potential sites of bone deficiencies.

2. Methods

2.1 Participants

A total of 257 children between the ages of 6–17 years were included in this analysis. Children were divided into three groups: typically developing children (control group, $n=167$), ambulatory children with spina bifida (AmbSB group, $n=80$), and non-ambulatory children with spina bifida (Non-AmbSB group, $n=10$). All children in the AmbSB and Non-AmbSB groups had been diagnosed with myelomeningocele, the most common and severe type of spina bifida in which the spinal cord protrudes outside the spinal column during fetal development. The average age, height, weight, sex and race characteristics for each group can be found in Table 1.

2.2 Image Acquisition

All participants were assessed by CT using the same scanner (Philips Gemini GXL, Philips Medical Systems Inc., Cleveland, OH) and the same mineral reference phantom for simultaneous calibration (Mindways Model 3 CT Calibration Phantom, Mindways Software, Inc., Austin, TX). The phantom was scanned at the same time as the bone and extended the entire length of the tibia. The same certified radiology technologist carried out all scans. With the subject lying supine, contiguous 1 mm slices were acquired at 90 kVp, 32 mA (100 mA for scout scan), and 1 s rotation time from knee to ankle joints. The scan field of view was 25 cm and the matrix resolution was 512×512 pixels. All images were acquired with a sharp point filter for distortion compensation and artifact reduction and a level B resolution filter; both are standard filters from Philips scanner software. These scanning parameters were set much lower than standard clinical CT settings to minimize radiation exposure; the effective radiation dose was estimated to be <0.05 mSv. Each CT scan was completed in approximately 5 min.

2.3 Image Processing

Each CT-image (DICOM format) sequence was imported into Osirix software [11] (Figure 1A) and a region of interest (ROI) containing only the right tibia was manually defined. For one non-ambulatory child with spina bifida, the left leg was analyzed instead of the right due to a previous fracture in the right leg. The tibial ROI was defined for each image in the stack between the proximal and distal tibia ends, and all pixel values outside the tibial ROI (including the fibula) were set to a background value of -1000 HU. The proximal end of the tibia was defined as the most proximal image slice where the intercondyloid eminence was first visible and the distal end was defined as the most distal image slice where the medial malleolus was visible. The isolated tibia images were imported into ImageJ software (1.47v). Noise was removed using a median filter with a radius of 1 pixel and a threshold of 50 for the raw pixel value (Figure 1B, Figure 1D).

Analysis of the bone was performed using an ImageJ plugin, BoneJ (version 1.3.11) [12]. BoneJ uses a thresholding method to identify bone and calculate bone properties. The lower limit HU threshold used for bone was 206 HU, and the maximum was left at the BoneJ default of 4000 HU. The lower limit corresponds with a density of $126.5 \text{ mg/cm}^3 \text{ K}_2\text{HPO}_4$ and was chosen to be low enough to capture both trabecular and cortical bone. A standard

conversion equation was used to convert CT Hounsfield Unit (HU) values to density (equivalent aqueous K_2HPO_4 mg/cm^3) based on the phantom calibration:

$$BMD = \frac{ROI \text{ Value (HU)} - BMD \text{ Intercept}}{BMD \text{ Slope}}$$

where BMD Intercept = 2.3 and BMD Slope = 1.6. This standard conversion equation was used in place of scan-specific conversions to facilitate integration with BoneJ. The BMD Intercept and BMD Slope constants represent the average slope and intercept determined from a sample of fifteen scans. To test for possible changes in the conversion due to scanner drift, the fifteen scans spanned the entire timespan of the study. Scan-specific conversion coefficients were calculated for each scan and used to calculate densities equivalent to the thresholds for trabecular bone (206 HU) and cortical bone (700 HU). The mean percent difference between the densities calculated using the standard and scan-specific calibrations was 1.4% and 1.0% for the 206 HU and 700 HU thresholds, respectively. This result indicated that variability in the scanner calibration throughout the time period of the study was reasonably low, and the use of a standard density conversion equation was appropriate.

To control for bone position relative to the scan plane, all tibias were aligned with their long axis using the moments of inertia function in BoneJ. A new stack was created by calculating the principle axes of inertia and aligning the tibia along the minimum axis. The realigned images retained the pixel height of the original image, and the voxel depth was adjusted to be equal to the pixel height. The aligned bone was re-sliced to a slice spacing equal to the image's pixel height. Pixel size varied minimally between images, with a difference of 0.486 mm between the maximum and minimum pixel height. The entire CT-image stack was then processed with the slice geometry function in BoneJ. This function computes the total area of all pixels with values above the 206 HU threshold chosen for bone. The resulting bone area (BA) is a measure of the total area of bone in each cross-section (Figure 1C, Figure 1E).

2.4 Calculating Density Weighted Bone Area Along the Length of the Tibia

The BoneJ slice geometry results and the isolated tibia images were imported into MATLAB (Mathworks Inc., Natick, MA) to perform size-normalization and calculate density weighted BA (DWBA). Normalized BA ($nBA = BA / \text{total bone length}^2$) and normalized length were calculated to compare bones of different sizes.

In order to determine the DWBA across the entire normalized length of the tibia, custom MATLAB code was written to weight the area of each pixel above the bone threshold (206 HU) by its pixel density. Pixel area was determined using the pixel height and width from the DICOM meta-data. For each individual image across the entire length of the bone, the DWBA was calculated as follows:

$$DWBA = \sum (\text{pixel area} * \text{density value for pixel} (\frac{mg}{cm^3}))$$

where only pixels greater than or equal to the $126.5 \text{ mg/cm}^3 \text{ K}_2\text{HPO}_4$ threshold were included in the summation. This DWBA provided an additional measure by providing an indication of the density of the calculated BA. In order to allow a comparison among children with varying bone sizes, the normalized DWBA (nDWBA) was then calculated as follows:

$$nDWBA = \frac{DWBSA}{length^2}$$

2.5 Representation of Bone Volume and Mass

The normalized length of the tibia was sectioned into three regions: the proximal epiphysis (0% to 20% of normalized length), the diaphysis (>20% to <80% of normalized length), and the distal epiphysis (80% to 100% of normalized length). The boundaries (20% and 80%) were chosen to approximate epiphyseal regions because the nBA changes drastically at these landmarks from large values of the epiphyses to smaller values of the diaphysis (Figure 2). By integrating the area under the nBA and nDWBA curves the normalized bone volume and normalized bone mass were calculated, respectively, for each of the three regions. The integrals of nBA and nDWBA provided a value representative of the entire bone volume and mass in the epiphyses and diaphysis.

2.6 Validation and Sensitivity Analysis of Threshold Method

To ensure validity of results, the BA calculated with our threshold technique was compared to results measuring bone area using a border finding command in MATLAB at 13%, 50%, and 90% of total bone length. The analysis was done on 15 children (5 per group). Comparison between our thresholding technique with a border finding algorithm showed a Pearson correlation coefficient of 0.91 at 13% of total bone length, 0.99 at 50% of total bone length, and 0.92 at 90% of total bone length.

Additionally, an analysis of sensitivity of results to the chosen threshold (206 HU) was completed. Normalized bone mass for a group of non-AmbSB children ($n=5$) and typically developing children ($n=5$) was calculated with thresholds of 186 HU and 226 HU. Sensitivity analysis indicated a Pearson correlation coefficient of 0.99 for comparison of both the 186 HU and 226 HU thresholds to the chosen threshold of 206 HU for both the metaphyses and the diaphysis.

2.7 Statistical Analysis

Analysis of variance (ANOVA) ($P < 0.05$) and Bonferroni post-hoc tests were used to evaluate differences in normalized bone volume and mass for each of the three bone regions (epiphyses and diaphysis) among the control, AmbSB and Non-AmbSB groups. All statistical analyses were performed using Stata (version 12.1, StataCorp LP, College Station TX).

3. Results

Figure 2 shows the nBA across the normalized bone length for one control child (7.8 years old). As expected, the epiphyseal regions have an increased nBA in comparison to the diaphyseal region. The variation and range of nBA values is much smaller in the diaphysis in comparison to the epiphyses. The growth plates in the epiphyses can be observed between the two nBA maxima in both the proximal and distal sites. The decreased nBA in the growth plate region reflects of our choice to define nBA as including only a bone-sectional area.

The results for the mean nBA and nDWBA of each group are shown in Figure 3. In comparison to the control group, there are similar values for nBA and nDWBA in the diaphysis and epiphyses for the AmbSB group. The Non-AmbSB group exhibits a lower nBA in the epiphyses and a lower nDWBA throughout the length of the tibia. The AmbSB group shows a slight reduction in nBA and nDWBA in the proximal epiphyseal region compared with the control group, but this reduction is not as great as that of the Non-AmbSB group.

Results for the mean normalized bone volumes of the epiphyses and diaphysis for the control, AmbSB, and Non-AmbSB groups are shown in Table 2 and Figure 4, along with P-values for comparison across all three groups. The mean normalized bone volume of the Non-AmbSB group was 39.3% lower than the AmbSB group and 44.4% lower than the control group in the proximal epiphysis ($P < 0.001$) and 31.7% lower than the AmbSB group and 33.3% lower than the control group in the distal epiphysis ($P < 0.001$). In the diaphysis, the Non-AmbSB group also had a mean normalized bone volume that was 17.4% less than the AmbSB group and 18.4% less than the control group ($P < 0.02$, $P = 0.01$). In comparison to the control group, the AmbSB group had a 8.3% lower mean normalized bone volume in the proximal epiphysis ($P = 0.02$), 2.4% lower mean normalized bone volume in the distal epiphysis ($P > 0.9$), and a 1.2% lower mean normalized bone volume in the diaphysis ($P > 0.9$). The percent difference between the epiphyseal bone volume of the Non-AmbSB group to the AmbSB and control groups is greater proximally than distally.

Results for the mean normalized bone mass of the epiphyses and diaphysis are shown in Table 2 and Figure 5, along with P-values for comparison across all three groups. Results indicate significantly lower normalized bone mass in the Non-AmbSB group compared with the control and AmbSB groups for both epiphyses and the diaphysis ($P = 0.001$). In comparison to the control and ambulatory groups, the Non-AmbSB group had a decrease in mean normalized bone mass of 66.5% and 64.5% in the proximal epiphysis, 60.7% and 60.8% in the distal epiphysis, and 45.4% and 48.7% in the diaphysis, respectively. In contrast to a small but significant difference in normalized bone volume of the proximal epiphysis, comparison of the control and AmbSB groups did not indicate statistically significant differences in normalized bone mass in the distal epiphysis ($P > 0.5$), proximal epiphysis ($P > 0.7$) or diaphysis ($P > 0.9$).

4. Discussion

To date, several studies have used DXA to measure BMD in the lower extremities of children with spina bifida. Past research using distal femoral DXA scans has shown that

children with spina bifida (especially those that are non-ambulatory) are prone to lower bone density at this site in comparison to typically developing peers [13]. In addition, this significant decrease in BMD is independent of fracture history [14]. DXA scans of children with different physical ability (ambulatory/non-ambulatory) and sport activity participation (sports active/non-active) reveal that BMD at the lumbar spine and femoral neck for children with myelomeningocele who engaged in physical activity was higher in comparison to peers with equivalent disabilities who did not engage in physical activity [15]. Results of this study also indicated that the observed lower BMD of all children was more prominent at the femoral neck, which has a high risk for pathological fractures.

The method presented here provides additional information in comparison to these studies. By analyzing bone mass along the whole length of the tibia, it is evident that the significant differences in tibial bone mass between the Non-AmbSB group and the control and AmbSB groups can be seen throughout the entire length of the tibia. This finding should be an important consideration when assessing bone mass in children with spina bifida. If there is a limitation that prevents the scanning of the whole length of a bone, scanning the proximal epiphysis may provide a better representation for determining the degree of decreased BMD, since this is the region that shows the greatest percent difference in BMD. Furthermore, analyzing one slice of bone of the midshaft may not be sufficient for determining all the information about decreases in bone mass for different regions.

Our results indicate significantly decreased bone mass in the tibia within the Non-AmbSB group. The observed decrease in bone mass throughout the length of the tibia may indicate a potential increase in tibial fracture risk in the non-ambulatory pediatric spina bifida population. The greater deficits of bone mass in the epiphyses may explain the high prevalence of tibial fractures seen in the pediatric spina bifida population at these sites, which has been reported at rates of up to 12.2% [4]. It has been reported that there is a higher incidence of distal than proximal tibial fractures [4]. However, our results indicate greater decreases in bone mass proximally, which would seem to indicate that the proximal tibia would be more susceptible to fracture. Therefore consideration of our results and the finding of higher incidence of distal tibial fractures suggest that additional factors aside from decreased bone mass influence fracture. Possible additional factors include greater loading at the distal tibia, but this would have to be confirmed in future studies. Ambulatory children with spina bifida had nDWBA values close to typically developing children and bone mass values that were not significantly different, suggesting that even a limited amount of ambulation may help build and maintain bone mass in this population despite decreases in normalized bone volume. The relative contributions of bone density and bone volume are not evident from DXA scans.

One limitation to this study is the selection of a bone threshold that is lower compared to a previous study using 150 equivalent aqueous K_2HPO_4 mg/cm³ to capture trabecular bone [16]. By selecting a fairly low bone density threshold of 126.5 equivalent aqueous K_2HPO_4 mg/cm³ in order to capture trabecular bone in its entirety, this study analyzed a bone volume and bone mass that accounted for both cortical and cancellous bone. While the threshold affects the measured bone area, it should have a similar effect across all participants. Since the focus of this study was a comparison between groups, the threshold of 126.5 equivalent

aqueous K_2HPO_4 mg/cm^3 was deemed acceptable, as it will not impact the relative comparisons. Furthermore, our validation and sensitivity analyses on thresholding levels and thresholding techniques show that the measurements of bone volume and bone mass are highly correlated and that all groups are affected similarly. However, the thresholding procedure has a greater impact on measurements of trabecular bone than on cortical bone. This limitation should be taken into account when considering comparisons between the epiphyseal and diaphyseal regions. In addition, future work should also include applying a more robust filter (such as a Gauss filter) before the thresholding process to better reduce the effects of high frequency noise.

Another limitation of this study is that only one leg was analyzed for each patient. Since some patients with spina bifida exhibit asymmetry in strength and function, future work will analyze bone mass and bone volume on both legs for patients for whom asymmetry in bone measurements is expected. Finally, although BA and bone length were normalized, patients included in this study were at various development stages. Future work should include analyses that account for other measures of growth such as weight, body mass index, and skeletal or sexual maturity (Tanner stage), which will provide additional information on factors that influence bone volume and bone mass.

Strengths of this study include analysis of a large sample size. It also provides insight into a method for analyzing the entire length of a long bone with the use of CT-images, thereby providing new information on bone mass and bone volume deficiencies that is not available from prior analyses based on DXA. In addition, our method allows a comparison of bone volume and bone mass that takes into account differences in bone size due to age. By normalizing bone length and area, we decrease the impact of differences in volume or density due to age and create a more equitable comparison of groups with children in different stages of development.

The method described here uses CT-images to determine the integrals of nBA and nDWBA as a representation of bone volume and mass across the entire length of the tibia. This approach to quantify CT scans has potential applications in all populations. This method addresses the current limitations of bone density measurements by providing a means for standardizing bone size and shape and measuring bone density along the entire length of a peripheral long bone. In addition to calculating BA and DWBA of the tibia, this method can also be applied to other long bones and expanded to determine additional mechanical parameters, such as moment of area or section modulus. Analyzing moment of area would provide insight into spatial distributions of bone mass within a given cross-section, which is not represented with our analysis of bone mass alone.

5. Conclusion

This method allows for analysis of the entire length of a bone and provides insight into the locations of greatest deficit in bone volume and bone mass. Although applied to the spina bifida population, this method has important clinical applications as a diagnostic tool for all patients with osteoporosis, osteopenia and/or paraplegia. For the pediatric population with spina bifida, knowing the severity and location of bone mass and bone volume deficiencies

can allow for development of therapies to target these sites specifically. For example, even a limited amount of walking appears to be beneficial for building bone mass and volume in this population, particularly in the epiphyses (trabecular bone sites). These findings may apply more broadly to other patient populations with impaired ambulation, but future research is needed to confirm whether a limited amount of ambulation can maintain bone mass in other patient populations.

Acknowledgments

Support provided by NIH-NICHD Grant # 5R01HD059826.

References

1. Quan A, Adams R, Ekmark E, Baum M. Bone mineral density in children with myelomeningocele. *Pediatrics*. 1998; 102:E34. [PubMed: 9724682]
2. Drummond DS, Moreau M, Cruess RL. Post-operative neuropathic fractures in patients with myelomeningocele. *Dev Med Child Neurol*. 1981; 23:147–150. [PubMed: 7215705]
3. Marreiros H, Monteiro L, Loff C, Calado E. Fractures in children and adolescents with spina bifida: the experience of a Portuguese tertiary-care hospital. *Dev Med Child Neurol*. 2010; 52:754–759.10.1111/j.1469-8749.2010.03658.x [PubMed: 20345948]
4. Parsch K. Origin and treatment of fractures in spina bifida. *Eur J Pediatr Surg Off J Austrian Assoc Pediatr Surg Al Z Für Kinderchir*. 1991; 1:298–305.10.1055/s-2008-1042509
5. Marreiros H, Marreiros HF, Loff C, Calado E. Osteoporosis in paediatric patients with spina bifida. *J Spinal Cord Med*. 2012; 35:9–21.10.1179/2045772311Y.0000000042 [PubMed: 22330186]
6. Bachrach LK. Osteoporosis and measurement of bone mass in children and adolescents. *Endocrinol Metab Clin North Am*. 2005; 34:521–535. vii.10.1016/j.ecl.2005.04.001 [PubMed: 16085157]
7. Bachrach LK. Consensus and controversy regarding osteoporosis in the pediatric population. *Endocr Pract Off J Am Coll Endocrinol Am Assoc Clin Endocrinol*. 2007; 13:513–520.10.4158/EP.13.5.513
8. Specker BL, Schoenau E. Quantitative bone analysis in children: current methods and recommendations. *J Pediatr*. 2005; 146:726–731.10.1016/j.jpeds.2005.02.002 [PubMed: 15973307]
9. Rosenblum MF, Finegold DN, Charney EB. Assessment of stature of children with myelomeningocele, and usefulness of arm-span measurement. *Dev Med Child Neurol*. 1983; 25:338–342. [PubMed: 6873495]
10. Sheridan KJ. Osteoporosis in adults with cerebral palsy. *Dev Med Child Neurol*. 2009; 51(Suppl 4):38–51.10.1111/j.1469-8749.2009.03432.x [PubMed: 19740209]
11. Rosset A, Spadola L, Ratib O. OsiriX: an open-source software for navigating in multidimensional DICOM images. *J Digit Imaging*. 2004; 17:205–216.10.1007/s10278-004-1014-6 [PubMed: 15534753]
12. Doube M, Kłosowski MM, Arganda-Carreras I, Cordelières FP, Dougherty RP, Jackson JS, et al. BoneJ: Free and extensible bone image analysis in ImageJ. *Bone*. 2010; 47:1076–1079.10.1016/j.bone.2010.08.023 [PubMed: 20817052]
13. Szalay EA, Cheema A. Children with Spina Bifida are at Risk for Low Bone Density. *Clin Orthop*. 2011; 469:1253–1257.10.1007/s11999-010-1634-8 [PubMed: 21042897]
14. Apkon SD, Fenton L, Coll JR. Bone mineral density in children with myelomeningocele. *Dev Med Child Neurol*. 2009; 51:63–67.10.1111/j.1469-8749.2008.03102.x [PubMed: 18811711]
15. Ausili E, Focarelli B, Tabacco F, Fortunelli G, Caradonna P, Massimi L, et al. Bone mineral density and body composition in a myelomeningocele children population: effects of walking ability and sport activity. *Eur Rev Med Pharmacol Sci*. 2008; 12:349–354. [PubMed: 19146196]
16. Manske SL, Liu-Ambrose T, Cooper DML, Kontulainen S, Guy P, Forster BB, et al. Cortical and trabecular bone in the femoral neck both contribute to proximal femur failure load prediction.

Osteoporos Int J Establ Result Coop Eur Found Osteoporos Natl Osteoporos Found USA. 2009;
20:445–453.10.1007/s00198-008-0675-2

Author Manuscript

Author Manuscript

Author Manuscript

Author Manuscript

- We present a method of quantifying bone mass along the entire length of a long bone
- The methodology is based on the analysis of CT scans
- We present results for ambulatory and non-ambulatory children with spina bifida
- These results are compared to typically developing children
- Results indicate that even limited ambulation may help build and maintain bone mass

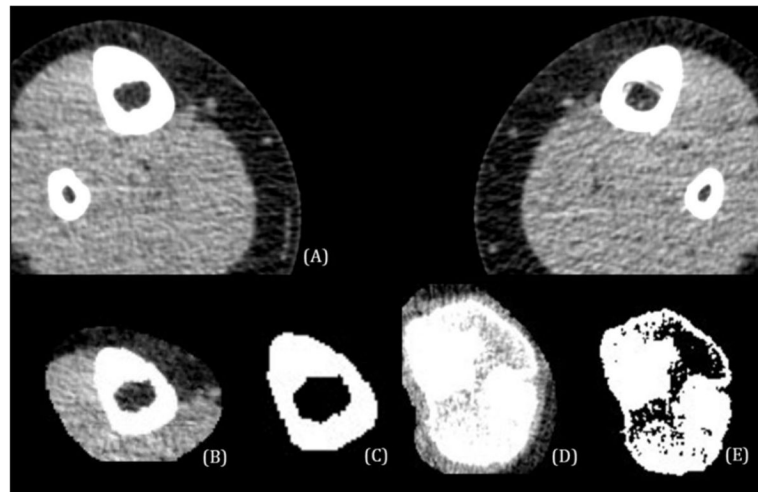


Figure 1.

A) CT-image of a control child before image processing; B) An ROI has been defined in the diaphysis and the same CT-image slice has been filtered to remove noise, and aligned in BoneJ; C) This image illustrates the application of the 206 HU threshold on the CT-image in (B); D) An ROI has been defined in the proximal epiphysis and the same CT-image slice has been filtered to remove noise, and aligned in BoneJ; E) This image illustrates the application of the 206 HU threshold on the CT-image in (D).

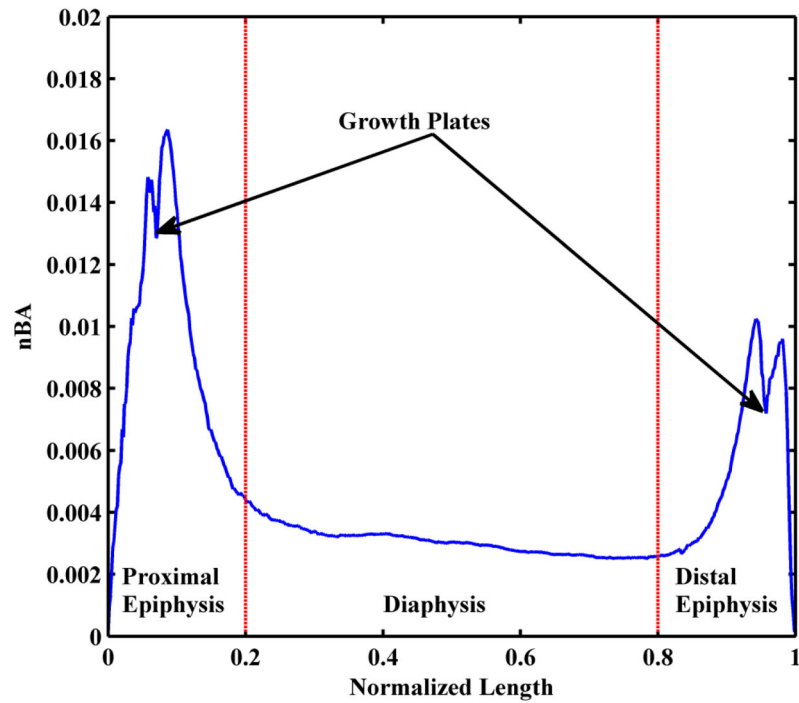


Figure 2. Normalized bone area (nBA) of a control child (7.8 years old) across the entire normalized length of the tibia. The epiphyseal and diaphyseal regions are labeled as well as the growth plates in the epiphyses.

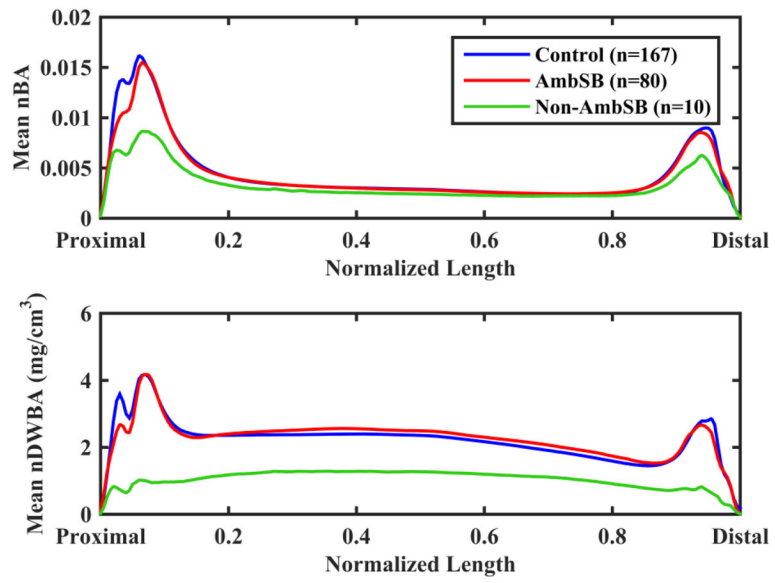


Figure 3. Mean normalized bone area (nBA) and normalized density-weighted bone area (nDWBA) across normalized slice position for the control, AmbSB and Non-AmbSB groups.

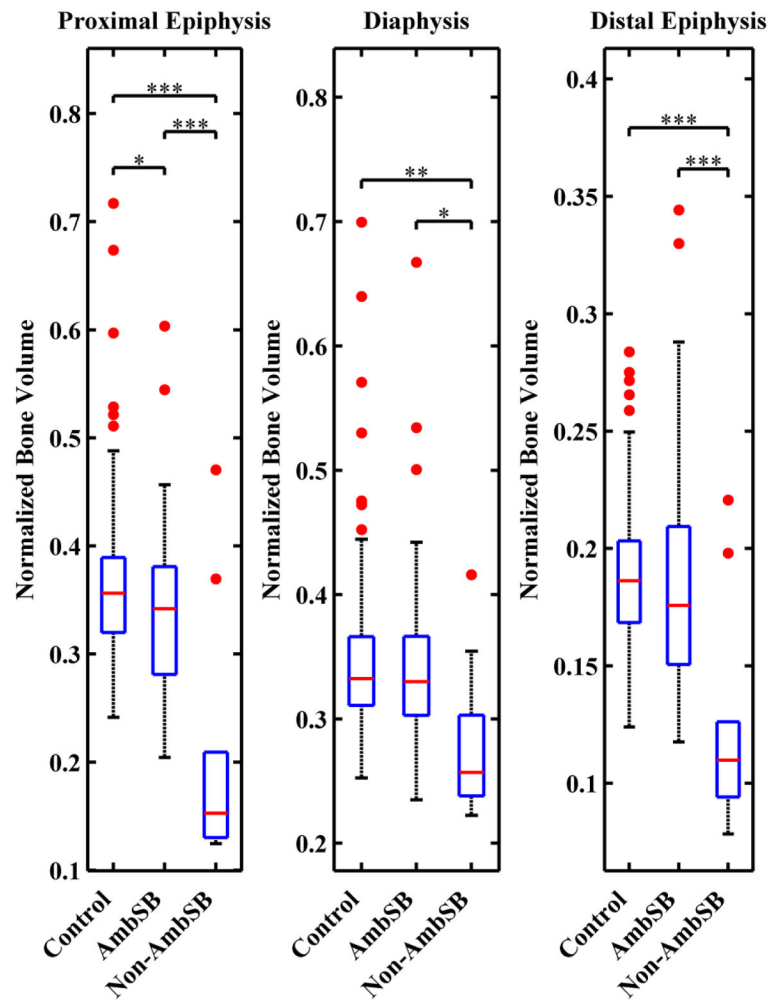


Figure 4.

The integral of normalized bone area (nBA) as a representation of normalized bone volume in the epiphyses and diaphysis. For each group, boxplots show the median (red line), 25th and 75th percentiles (lower and upper edges of blue box), maximum and minimum non-outliers (whiskers) and outliers (red points). Data points are considered outliers if they greater than $[q_3 + 1.5(q_3 - q_1)]$ or smaller than $[q_1 - 1.5(q_3 - q_1)]$, where q_3 and q_1 and the 75th and 25th percentiles respectively. Brackets above the boxplots indicate statistically significant differences between control, AmbSB and Non-AmbSB groups (* P 0.05, ** P 0.01, *** P 0.001).

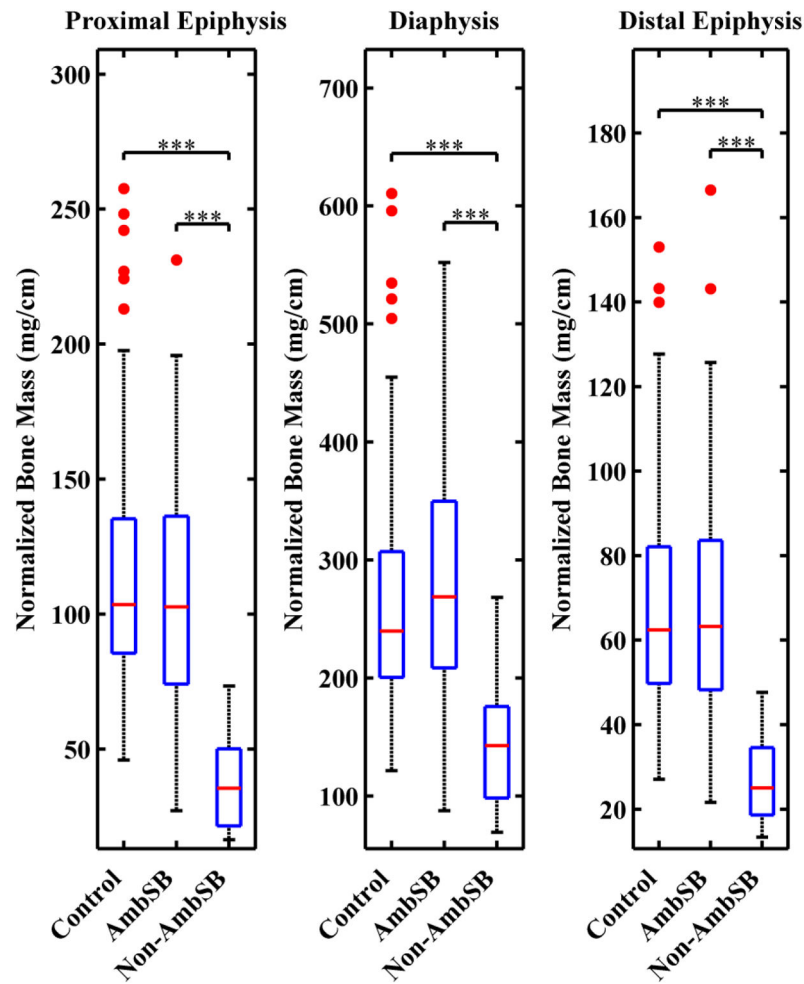


Figure 5.

The integral of normalized density-weighted bone area (nDWBA) as a representation of normalized bone mass in the epiphyses and diaphysis. For each group, boxplots show the median (red line), 25th and 75th percentiles (lower and upper edges of blue box), maximum and minimum non-outliers (whiskers) and outliers (red points). Data points are considered outliers if they greater than $[q_3 + 1.5(q_3 - q_1)]$ or smaller than $[q_1 - 1.5(q_3 - q_1)]$, where q_3 and q_1 and the 75th and 25th percentiles respectively. Statistically significant differences between control, AmbSB and Non-AmbSB groups are shown (***) $P < 0.001$.

Table 1

Means and standard deviations of age, height, and weight for the three study groups, as well as percent Hispanic and gender characteristics of the participants.

Mean (SD)	Control Group (<i>n</i> =167)	AmbSB Group (<i>n</i> =80)	Non-AmbSB Group (<i>n</i> =10)
Age (years)	12.0 (3.1)	9.7 (2.6)	12.8 (2.2)
Height (cm)	150.4 (17.3)	129.7 (17.3)	133.0 (13.4)
Weight (kg)	47.8 (17.3)	37.4 (18.8)	53.5 (19.4)
Race, n (%) Hispanic	110 (65.9%)	75 (93.8%)	10 (100.0%)
Gender, n (%) Male	90 (53.9%)	44 (55.0%)	8 (80.0%)

Author Manuscript

Author Manuscript

Author Manuscript

Author Manuscript

Table 2

The mean and standard deviations of the normalized bone volume and mass of the tibial epiphyses and diaphysis are shown. Bone volume was calculated from the integral of nBA and bone mass was calculated from the integral of nDWBA. *P*-values are included for the comparisons between groups.

	Control Group (<i>n</i> =167)	AmbSB Group (<i>n</i> =80)	Non-AmbSB Group (<i>n</i> =10)	<i>P</i> -value
Proximal Epiphysis				
Bone Volume	0.36 (0.07)	0.34 (0.07) ^{<i>a</i>}	0.20 (0.12) ^{<i>a,b</i>}	0.001
Bone Mass (mg/cm)	112.5 (40.5)	106.2 (42.0)	37.7 (18.4) ^{<i>a,b</i>}	0.001
Distal Epiphysis				
Bone Volume	0.19 (0.03)	0.18 (0.04)	0.12 (0.05) ^{<i>a,b</i>}	0.001
Bone Mass (mg/cm)	67.7 (24.2)	67.6 (28.3)	26.6 (10.4) ^{<i>a,b</i>}	0.001
Diaphysis				
Bone Volume	0.34 (0.06)	0.34 (0.06)	0.28 (0.06) ^{<i>a,b</i>}	0.01
Bone Mass (mg/cm)	262.3 (87.9)	279.0 (104.6)	143.1 (56.4) ^{<i>a,b</i>}	0.001

^{*a*} denotes a significant difference from the control group

^{*b*} denotes a significant difference from the AmbSB group